

論文題目 **Development of Superconducting Transition Edge Sensor Microcalorimeters**
(超伝導転移端センサマイクロカロリメータの開発)

氏 名 ラスナヤカ ムディヤンセラゲ , トウシャラ ダマヤンティ

1. Introduction

Superconducting Transition Edge Sensor (TES) microcalorimeters are promising energy resolving detectors of single photons from the far infrared, optical, X-ray through gamma rays and sensitive detectors of photon fluxes out to millimeter wave lengths. A microcalorimeter is basically a thermal detector consists of an absorber, a thermometer and a low temperature heat sink. The key difference between TES detectors and other thermal detectors is the superconducting thermometer, which is operating at very low temperatures (normally below 0.1K). Superconducting transition can be extremely sharp, making a very sensitive thermometer.

Theoretical energy resolution limit of TES detector is $\sim 1\text{eV}$ full width at half maximum (FWHM). TESs have been developed more than over a decade for X-ray spectroscopy and well established with an ultra high energy resolution of 1.8 eV at 6 keV with a Mo/Au TES¹. In our laboratory also, we have been developing TES detectors in X-ray band and the best energy resolution so far is 9.4 eV with an Ir/Au bilayer TES². However, TES detectors are still under development in the infrared range (low energy extreme) and for gamma ray spectroscopy (high energy extreme). Therefore we are motivated to pursue our studies on these two energy extreme measurements.

2. Development of a TES single photon counter

In the low energy extreme there is a big demand for true single photon number resolving detectors for novel quantum information applications. NIST group of USA has been developed a high quantum efficient (88%), single photon resolving detector with a tungsten (W) TES³. However, low speed of their detector (~ 50 kHz) is not sufficient for many quantum information applications. I worked with AIST (Advanced Institute for Industrial Science and technology, Japan) research group to develop a fast response, high quantum efficient (QE) single photon counter (SPC) to fulfill the requirements of quantum information fields.

Detector

The response time will be improved at high operating temperature. Ti is one of ideal candidate with transition temperature, $T_c \sim 390$ mK. And another benefit of Ti over W is Ti has a lower optical reflectance of $\sim 65\%$, compared to $\sim 84\%$ of W at 1550 nm that will enhance the QE. Therefore we choose Ti for our SPC. The Ti-TES devices were fabricated at AIST Nano processing Facilities (AIST-NPF). Fig. 1 shows a microscopic view of the four Ti-TES devices. Ti films are squares of side of 20 μm (upper) and 10 μm (lower) with a thickness of 46 nm. Electrical contacts are provided through 90 nm thick Nb leads.

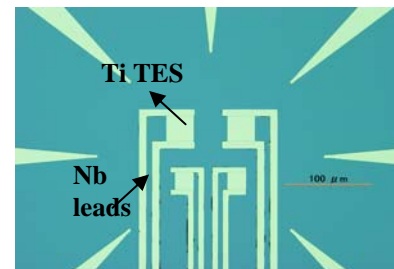


Fig. 1 microscopic view of four Ti-TES detectors.

Experimental

This detector was tested at the cold stage (~ 320 mK) of a ^3He refrigerator and irradiated from 1550 nm optical photons (energy ~ 0.8 eV) through a single mode optical fiber placed ~ 100 μm from the TES. The Ti-TES was voltage biased with a 0.5 Ω shunt resistance and current through the TES was read by a 200-series arrayed SQUID current amplifier. This device showed the superconductivity at 358 mK. Measured current signals from this detector have a rise time and fall time of 30 ns and 313 ns. Fig. 2 shows the first single photon discrimination results of

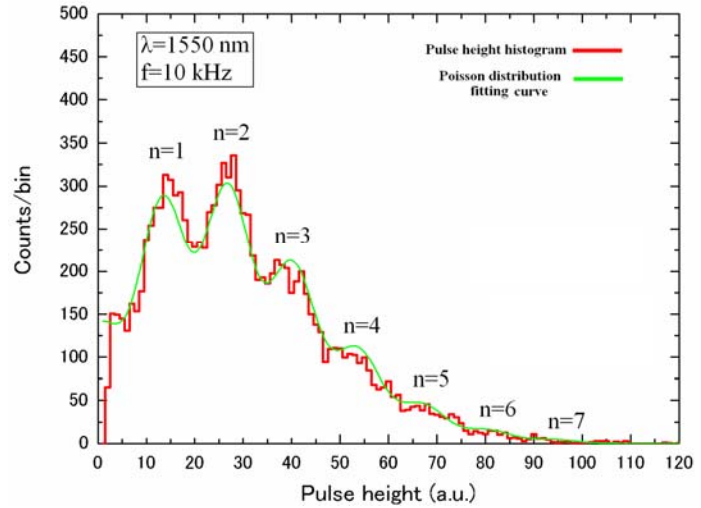


Fig. 2 Pulse height histogram for 1550 nm laser illumination (red) with its Poisson distribution fitting curve (green).

Ti-TES for highly attenuated 1550 nm laser illumination. At the first stage, Ti-TES has resolved up to seven photons.

By fitting the measured spectrum with a Poisson distribution, which fitting line is shown in the spectrum, we obtain the ER of 0.69 eV FWHM and QE of $\sim 5\%$. Single photon resolving capability with a very fast signal response that is ten times faster than currently existing devices is very promising for high speed single photon detection. By improving the QE of this detector will be more powerful for various quantum information applications.

Optical absorption cavity design for Ti-TES

QE is mainly limited by the high reflectance at the Ti film. By embedding the Ti-TES in optical photon absorption cavity to reduce both the reflection and transmission of optical photons through Ti film will effectively improve the QE of the detector.

To simulate a structure, first we obtained the refractive index of our fabricated Ti films using an ellipsometer. Using TFCalc simulation software we designed an absorption cavity for Ti, which is optimized for 1550 nm. The simulated cavity structure incorporates the Ti in a stack of elements on a Si substrate, which is shown in the inset of Fig. 3. In Fig. 3 the solid line shows the simulated reflectance curve and the dashed line shows the measured reflectance curve of the cavity structure.

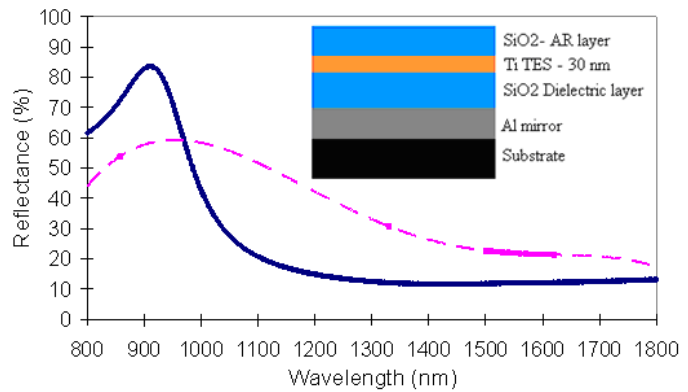


Fig. 3 Simulated (solid) and measured (dashed) reflectance curves of the cavity structure shown in inset.

While simulation results show $\sim 12\%$ optical reflectance, experimental results show $\sim 21\%$ reflectance at 1550 nm. Disagreement of simulation and measured values can be attributed to the stray light effect from background. Our calculations shows an absorption $> 75\%$ for the cavity structure.

AIST group has successfully fabricated the optical TES using this optical cavity, and obtained the fast rise time and fall time of 40 ns and 190 ns, respectively, with an ER of 0.49 eV and QE of 64% . These

results confirm the performances of Ti-TES embedded in an optical cavity structure.

Encouraged from successful results in the low energy extreme, we think to move to the high energy extreme.

3. Development of a TES gamma ray detector for CDB-PAS analysis

In the high energy extreme, we are interested of Coincidence Doppler Broadening Positron Annihilation Spectroscopy (CDB-PAS), which is a well established technique to detect defect of materials. Specific application area is to analyze the defects of nuclear reactor pressure vessels, which results from neutron irradiation during reactor operation. High purity germanium (HPGe) detectors are currently used for these analyses. However, their energy resolution is limited to $\sim 1\text{keV}$ at $\sim 511\text{keV}$ and not sufficient for precision analysis. On the other hand, TESs have been developed for gamma ray spectroscopy with more than an order of better energy resolution than HPGe detectors⁴. However, TES gamma ray detector development has been limited up to $\sim 100\text{keV}$ range due to the requirement of thick absorbers to stop higher gamma ray photons. This makes the fabrication difficulties and after mounting a large absorber on to a thin film TES, compound detector become weak and we have to manipulate the detector very carefully. We took this challenging issue to design and develop a TES gamma ray spectrometer with an energy resolution $\sim 500\text{eV}$, to apply for precision analysis of CDB-PAS.

Detector

Although Sn is widely used for TES gamma ray detectors in $\sim 100\text{keV}$ range, Pb provide more benefits over Sn at higher energies. We use $1\text{mm} \times 1\text{mm} \times 0.75\text{mm}$ bulk Pb absorbers with $C \sim 67\text{pJ/K}$ for our gamma-ray TES detector. Here, TES is a Ir/Au bilayer film of square of side $200\mu\text{m}$ fabricated on a 400nm thick SiN membrane with $G = 310\text{pW/K}$. The thicknesses of the Ir and Au films of 100nm and 25nm respectively results a $T_c \approx 110\text{mK}$. Electrical contacts are provided through 270nm thick Nb leads. TES devices were fabricated at the VLSI design and education center (VDEC), the University of Tokyo. The Pb absorber is thermally well coupled to the TES by a 0.0004cm^2 area, $\sim 50\mu\text{m}$ thick Stycast 2850FT epoxy layer, in which thermal conductivity is $\sim 16\text{nW/K}$. Cross sectional view of the detector is shown in Fig. 4.

Experimental

This detector was tested on the cold stage (64mK) of a dilution refrigerator. After attaching the absorber with Stycast the T_c dropped to $\sim 95\text{mK}$. The detector was irradiated from a ^{137}Cs source that produces

662keV gamma rays. Fig. 5 shows the recorded spectrum, with the full energy

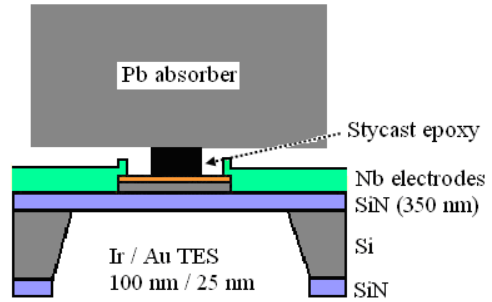


Fig. 4 Cross sectional view of TES gamma ray detector.

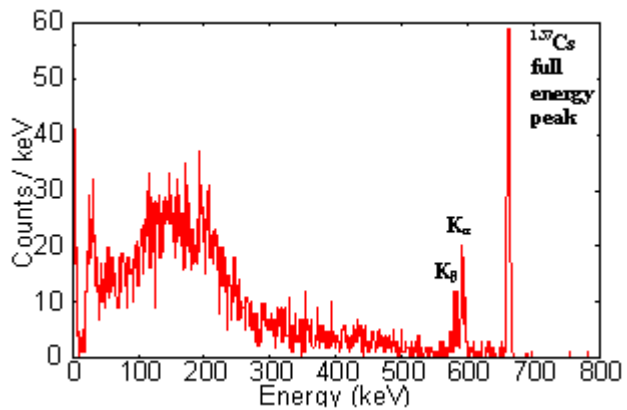


Fig. 5 Energy spectrum recorded from 662keV gamma rays emitted by a ^{137}Cs source showing the photoelectron absorption peak and Pb K_α and K_β escape peaks.

peak of FWHM ER of 4.7 keV (0.7%) and the Pb K_{α} and K_{β} X-ray escape peaks (75 and 85 keV below the photopeak). As an additional characterization, we illuminated the detector with a ^{60}Co source and a successful energy spectrum was recorded with FWHM ER of 2.9 keV (0.2%) at 1173 keV. Energy resolution of the detector is still far from our requirements.

Measured baseline noise (1.56 keV) has a large contribution to degrade the energy resolution. Compound model analysis shows that the inherent noise of detector itself has only 33 eV contributions to the noise. This means that the noise of SQUID and bias circuit may effectively contribute to increase baseline noise. Energy resolution degradation is dominated by extra noise sources affected by temperature fluctuations of the cryostat, mechanical vibrations of the circulating system, external magnetic field, and some unknown noise components. By controlling these extra noise components and the noise of bias circuit energy resolution can be improved.

Measured current pulses have a ~ 150 μs rise time and a 140 ms fall time. The decay curve is fitted with two distinct time constants, a fast component of 3.1 ms followed by a very slow component of 135 ms. The fast component corresponds to the time constant of energy flowing out of the absorber through the epoxy, given by $C_{\text{abs}}/G_{\text{epoxy}} \approx 4$ ms. The mismatch is due to the uncertainty of thickness of epoxy layer. Heat capacity of this composite detector is ~ 70 pJ/K. This results a very slow C/G natural time constant of ~ 225 ms. Experimental results showed that the sensitivity of superconducting transition is limited to ~ 3.8 , resulting an effective decay time constant of ~ 132 ms, which corresponds to experimental decay time. Poor thermal sensitivity of the TES may be due to the stress of epoxy layer on the TES. We use SPICE simulation to analysis the device response time. Our simulation results show that the most practical way to improve response time is by increasing thermal conductivities from absorber to TES and from TES to heat sink.

4. Summary and conclusions

In the low energy extreme, we developed a high quantum efficient, sub-MHz count rate photon number resolving detector with a Ti-TES, which is promising to be applied in various quantum information applications. The performances of this Ti-TES are among the best measurements in this field.

In the high energy extreme, we could successively design a detector to resolve high energy gamma photons (>500 keV) using a bulk lead absorber mounted TES. Although energy resolution is still far from the requirements these are the first measurements at these energies with a TES detector. We understand that by improving the detector fabrication and measurement setup we can reach high energy resolution with a TES detector at high energy extreme too.

Therefore, now we are fabricating detectors using a flip chip bonder to mount the absorber on to the TES, to control the amount of epoxy and to reduce the stress on TES. Also we have already prepared a new experimental setup using an Adiabatic Demagnetization Refrigerator (ADR). Once the fabrication improvements have been implemented, and with the use of ADR for measurements, we expect that our Pb absorber mounted TES detector will achieve a high energy resolution, and will be a future challenge to commercial HPGe detector for CDB-PAS analysis.

References

1. S. R. Bandler et al., *J Low Temp Phys.*, **151**, 400 (2008).
2. Y. Kunieda et al., *Jpn. Jour.Appl. Phys.*, **43 (5A)**, 2742 (2004).
3. D. Rosenberg et al., *IEEE Trans. on Appl. Supercon.*, **15 (2)**, 575 (2005).
4. W.B.Doriese et al., *Appl. Phys. Lett.*, **90**, 193508 (2007).